MODELING HIGHLY SIDEROPHILE ELEMENT ABUNDANCES IN GROUP IIAB IRON METEORITES. J. E. Dietderich[1] and R. J. Walker[2], [1]Dept. of Earth and Atmospheric Sciences, Univ. Houston, Houston, TX 77204 (jedietderich@uh.edu), [2]Dept. of Geology, Univ. Maryland, College Park, MD 20742.

Introduction: The highly siderophile elements (HSE: including Re, Os, Ir, Ru, Pt, and Pd)) are useful for modeling processes of core formation in asteroids and planetesimals because of their high relative abundances in metal phases, and the fact that each element is fractionated differently between solid metal and liquid metal during core solidification. Here, we collected new HSE abundance data for group IIAB iron meteorites, and used this information to model fractional crystallization for each of the measured HSE (e.g., [1]).

This project is an extention of a previous study of both the isotopic and elemental systematics of IIAB irons [2]. The previous models of fractional crystallization for group IIAB were modified to consider the larger suite of HSE presented here.

Samples: The IIAB group has the second largest number of identified iron samples, and overall has the lowest nickel content of any of the major iron meteorite groups. The IIAB samples available for this study were inventoried and organized by Ni content, and a total of 15 samples were selected that span that compositional range of the group. Sample masses ranged from 25 mg, for the highest Ir abundance sample, to 372 mg, for the lowest Ir abundance sample.

Methods: The samples were cleaned of oxidation via abrasion and cleaned further in an ultrasonic ethanol bath, before being weighed on an electronic balance. Appropriate amounts of a mixed HSE spike were weighed out for each sample [2]. After being weighed, the spike was combined with the sample and an acid mixture (5 mL conc. HNO_3 and 3 mL conc. HCl), then sealed in Pyrex Carius tubes, and placed in an oven set to 240°C for a 24-hour period. After removal from the oven, the samples were packed in ice to prevent Os evaporation, and then moved from Carius tubes to centrifuge tubes for Os extraction.

Each sample was then mixed with CCl_4 and shaken to separate the Os from the iron matrix and other HSE. The dense CCl_4 was then extracted via a disposable pipetter, and deposited in a Teflon vessel containing conc. HBr. The extracted Os was further purified via microdistillation by re-oxidizing the sample with CrO_3, allowing the Os to transfer to a HBr droplet in a sealed, conical bottom Teflon vessel. The acid solution containing the remaining HSE was processed through anion exchange columns to separate the HSE into three groups (Re-Ru, Pt-Ir, and Pd).

Analysis of Os was performed using a *VG Sector 54* TIMS, and the concentrations were obtained via isotope dilution. Two ICP-MS instruments (a *Nu Instruments, Nu Plasma* and *ThermoElectron, Element 2*) were used on the remaining HSE, and again, the concentrations were obtained via isotope dilution.

The mass spectrometric analytical uncertainties from in-run statistics ranged from a low 0.1% for Os ratios achieved with the TIMS, to 0.2% for the Nu-Plasma ratios, and 0.5% for the ratios on the Element 2 (except for Pd that was 0.7%). Error magnification was empirically determined for each element in all samples. Some of the irons with the most highly fractionated HSE patterns show large errors in some elements. This is the result of error magnification resulting from the over spiking of low abundance elements. A new mixed spike is being created to circumvent this problem. Sample heterogeneity also had an impact on uncertainty, which was larger when working with the least Ir abundant samples. The total uncertainties, along with the concentration data are provided in **Table 1**.

Results: All data are reported in **Table 1** and then normalized to chondritic values (**Fig. 1**).

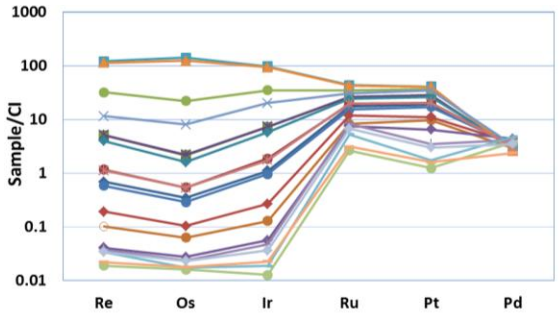

Figure 1. CI chondrite normalized abundances of HSE for IIAB irons.

Rhenium, Os, Ru, Pt, and Pd abundance data were plotted versus Ir data for high and low Ir abundance IIAB irons. Old Woman was selected as the midpoint between high and low Ir abundances. Two sets of linear regression lines were then obtained for the data in order to create a two stage model for calculated relative D values. The slopes of these linear regressions were used to calculate distribution coefficients for some of the HSE (Re, Os, Ru, Pt, Pd) relative to Ir. Palladium *D* values were also obtained from parameterizations.

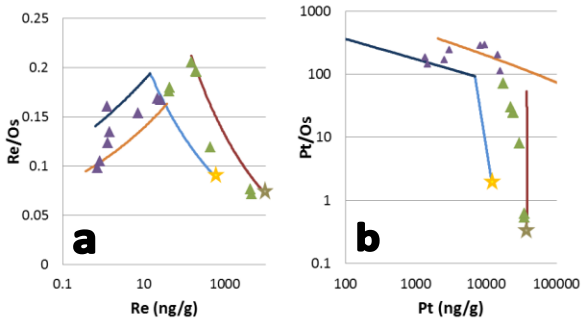

Figure 2a. Log-log plot of Re/Os ratios versus Re. **b.** Log-log plot of Pt/Os ratios versus Pt. The yellow/brown stars indicate the starting composition of the liquid/solid phases. As fractional crystallization progresses, each phase follows its respected track (liquid is blue/solid is red). At 26% crystallization the model begins to use the *D* values for low Ir abundance (liquid is dark blue/ solid is orange). The green/purple triangles represent the high/low Ir abundant data.

Discussion: With extensive research into crystallization systems [4] and a focus on Ir, the D_0 (the initial distribution coefficient), and initial weight percent S for group IIAB irons were estimated. Using those values, along with the calculated linear regression slope values, *D* values for each element (except Ir and Pd), for each step of fractional crystallization were determined using equations from [4,5].

Liquid and solid tracks that are consistent with the observed evolution of HSE abundances through crystallization were then calculated incrementally, and plotted with the collected abundance data. The two best representations of these models are provided in **Fig. 2a-b**. The presence of two solid tracks is caused by the restart of model calculations once 26% crystallization was reached.

The new crystal-liquid fractionation model accounted for mostg of the observed chemical variability in group IIAB iron meteorites. The model accounts for the observation of decreasing (Re, Os, Ir, Ru, and Pt) and increasing (Pd) concentrations during crystallization (**Fig. 1**). While similar elemental trends have previously been observed and documented for some HSE this is the first attempt to simultaneously model six HSE. Some problems remain. The greatest complexity and error in our model the result of the presumption of highly variable S and P abundances on the evolution of the metal compositions. Sulphur and P are incompatible elements in metal systems, and to some extent, similar to Pd, yet they have a major impact on HSE partitioning [4]. Nevertheless,even though the IIAB system is presumed to have had relatively high initial concentrationations of S and P, our results suggest that simple models can still account for most of the HSE data.

References: [1] Walker R. J. et al. (2008) *GCA, 72(8)*, 2198–2216. [2] Cook D. et al. (2004) *GCA, 68(6)*, 1413–1431. [3] Wasson J. et al. (2007) *GCA, 71(3)*, 760–781. [4] Chabot N. L. (2004) *GCA, 68(17)*, 3607-3618. [5] Chabot N. L. and Jones J. H. (2003) *Meteoritics & Planet. Sci., 38(10)*, 3607-3618.

Table 1. IIAB iron meteorite data (Ni content obtained from [3] / data marked w/ * = obtained from [2]).

Sample	Ni (%)	Re (ppb)	± (%)	Os (ppb)	± (%)	Ir (ppb)	± (%)	Ru (ppb)	± (%)	Pt (ppb)	± (%)	Pd (ppb)	± (%)
Negrillos	5.25	4623	0.75%	64460	1.2%	44520	1.3%	28100	0.64%	35100	0.75%	1454	1.1%
Bennett County	5.4	4340	0.68%	56840	0.95%	42800	1.1%	27940	0.61%	35000	0.71%	1465	1.1%
Gressk	5.57	439.5	0.60%	3698	0.67%	9200	0.90%	19770	0.74%	29940	1.0%	1876	0.88%
Filomena	5.5	197.2	0.29%	1010	0.26%	3319	0.31%	17110	0.35%	24550	0.49%	1606	0.22%
duplicate	5.6	192.7	0.28%	984.0	0.26%	3306	0.28%	16990	0.31%	24400	0.41%	1586	0.23%
Lombard	5.5	151.0	0.26%	735.2	0.26%	2627	0.28%	15620	0.32%	22350	0.44%	1730	0.25%
Old Woman B	5.49	44.51	0.27%	248.0	0.26%	849.3	0.29%	12650	0.54%	17560	0.83%	1838	0.30%
Old Woman A	5.63	42.90	0.65%	244.2	0.67%	797.3	0.70%	12840	1.3%	17490	2.0%	1753	1.0%
Navajo	5.49	26.17	0.30%	156.8	0.25%	503.4	0.25%	11300	0.33%	16010	0.44%	1838	0.25%
Mount Joy	5.78	22.15	0.29%	131.7	0.26%	435.5	0.29%	9899	0.73%	14690	1.2%	1880	0.39%
Bilibino	5.99	7.272	0.41%	47.45	0.31%	120.8	0.29%	7622	1.6%	9533	2.4%	2069	0.90%
Smithsonian Iron	5.55	3.888*	0.41%	28.56	0.29%	58.68	0.27%	5344	1.5%	8354	2.8%	1623	0.95%
Sikhote-Alin	6.03	1.429	0.85%	10.64	0.65%	21.13	0.55%	5400	8.6%	3010	6.8%	2330	10%
Derrick Peak	6.36	1.303	0.87%	10.56	0.67%	16.43	0.57%	4330	11%	2560	9.5%	1970	14%
Santa Luzia	6.04	1.278	0.81%	7.976	0.67%	8.463	0.45%	3400	9.8%	1470	6.4%	2690	18%
duplicate	6.04	0.8432	1.0%	8.039	0.66%	10.19	0.42%	2020	6.2%	1370	5.8%	1340	10%
São Julião de Moreira	5.78	0.7154	0.81%	7.285	0.68%	5.730	0.44%	1710	6.1%	1060	5.3%	2080	16%